Journal of Magnetic Resonance **156,** 161–170 (2002)
doi:10.1006/jmre.2002.2542

Optimized Pulse Parameters for Reducing Quantitation Errors Due to Saturation Factor Changes in Magnetic Resonance Spectroscopy

Craig J. Galbán and Richard G. S. Spencer[1]

National Institutes of Health, National Institute on Aging, GRC 4D-08, 5600 Nathan Shock Drive, Baltimore, Maryland 21224

Received March 16, 2001; revised April 4, 2002

We present an analysis of the effects of chemical exchange and changes in T_1 on metabolite quantitation for heart, skeletal muscle, and brain using the one-pulse experiment for a sample which is subject to temporal variation. We use an optimization algorithm to calculate interpulse delay times, TRs, and flip angles, θ, resulting in maximal root-mean-squared signal-to-noise per unit time (S/N) for all exchanging species under 5 and 10% constraints on quantitation errors. The optimization yields TR and θ pairs giving signal-to-noise per unit time close or superior to typical literature values. Additional simulations were performed to demonstrate explicitly the dependence of the quantitation errors on pulse parameters and variations in the properties of the sample, such as may occur after an intervention. We find that (i) correction for partial saturation in accordance with the usual analysis neglecting variations in metabolite concentrations and rate constants may readily result in quantitation errors of 15% or more; the exact degree of error depends upon the details of the system under consideration; (ii) if T_1's vary as well, significantly larger quantitation errors may occur; and (iii) optimal values of pulse parameters may minimize errors in quantitation with minimal S/N loss.

INTRODUCTION

^{31}P NMR studies of heart, skeletal muscle, and brain investigating the bioenergetic response to an intervention represent a common experimental paradigm in *in vivo* NMR. Specific interventions include exercise, electrical stimulation, ischemia, hypoxia, seizures in the case of brain, and administration of pharmacologic agents. Changes in pH and in the concentrations of phosphocreatine (PCr), ATP, and inorganic phosphate (P_i) can be quantitatively interpreted in terms of intracellular energy charge, aerobic threshold, and energy transduction efficiency, provided that metabolite levels are measured accurately. Accordingly, a tremendous amount of effort has been expended toward the goal of accurate quantitation, including development of optimized hardware, analysis routines, and pulse sequences.

A commonly used pulse sequence for quantitation is the one-pulse experiment, in which a long train of pulses of flip angle θ alternating with interpulse delays of duration TR is applied, with signal acquisition after each pulse. This experiment was proposed and analyzed by Ernst and Anderson (*1*). The Ernst equation gives the observed magnetization for a resonance line with a spin–lattice relaxation time, T_1,

$$\frac{M_{\text{obs}}(\theta, \text{TR})}{M_0} = \frac{(1 - e^{-\text{TR}/T_1})\sin\theta}{(1 - e^{-\text{TR}/T_1}\cos\theta)}, \qquad [1]$$

where M_0 is the equilibrium magnetization and $M_{\text{obs}}(\theta, \text{TR})$ is the observed magnetization in the steady state. The experimentally determined saturation factor, SF, is defined as the ratio of the observed magnetization to the equilibrium magnetization and, by the Ernst analysis, is a function of θ, TR, and T_1:

$$\text{SF}(T_1; \theta, \text{TR}) = \frac{M_{\text{obs}}(\theta, \text{TR})}{M_0}. \qquad [2]$$

According to Eqs. [1] and [2], the SF for each resonance in a multicomponent spectrum is entirely independent of the presence or properties of other resonances.

Improvements in the signal-to-noise ratio (S/N) can be achieved by acquiring data under saturating conditions. Ernst and Anderson (*1*) showed that for a given TR, the maximal S/N is achieved through selection of the flip angle, θ_E, according to

$$\cos(\theta_E) = e^{-\text{TR}/T_1}, \qquad [2.5]$$

where this optimal flip angle is conventionally known as the Ernst angle. The amplitude distortion resulting from saturation can be corrected using an empirical correction based on Eq. [2]. This requires that the SF be unchanged between the time it is measured and the time the saturated amplitude is measured. According to Eq. [1], this requires only that the T_1 be unchanged; however, more recent work (*2–6*) has shown that Eq. [1] is strictly valid only when the species under consideration is not in chemical exchange (CE). Otherwise, the SF has a functional dependence on all of the T_1's, M_0's, and rate constants within the reaction network.

In previous work (*3*) we quantitatively described the degree to which SFs are influenced by CE but did not address quantitation errors due to parameter, and hence SF, changes. Other work (*4*)

[1] To whom correspondence should be addressed.

1090-7807/02 $35.00

did address this, but only for a single illustrative example. The current manuscript presents a systematic exploration of errors due to changing parameters, including T_1 changes, for heart, skeletal muscle, and brain, as well as optimization procedures for decreasing these errors.

We examine the three-site system of PCr, γ-ATP, and P_i, with phosphate transfer mediated by the creatine kinase (CK) and ATP synthesis and hydrolysis reactions in heart, skeletal muscle, and brain:

$$\mathrm{PCr} \underset{k_{\gamma\text{-ATP}\to\mathrm{PCr}}}{\overset{k_{\mathrm{PCr}\to\gamma\text{-ATP}}}{\rightleftharpoons}} \gamma\text{-ATP} \underset{k_{\mathrm{P_i}\to\gamma\text{-ATP}}}{\overset{k_{\gamma\text{-ATP}\to\mathrm{P_i}}}{\rightleftharpoons}} \mathrm{P_i}. \qquad [3]$$

THEORY

Saturation Factors in the Presence of CE

We now summarize results of (*3*). As in the derivation of Eq. [1], full transverse relaxation during TR is assumed (*1*), as may be achieved by a sufficiently long TR or by application of homospoil pulses (*5, 6*). Then the general formula for SFs in the presence of CE amongst N species may be conveniently written in vector notation with vector element i corresponding to species S_i. With $\mathbf{M}_0$ and $\mathbf{SF}$ indicating the vectors of equilibrium magnetizations and SFs, respectively, and defining the matrix

$$\mathbf{M}_0 = \mathbf{I}\mathbf{M}_0, \qquad [4]$$

where $\mathbf{I}$ is the $N \times N$ identity matrix, one has

$$\begin{aligned}\mathbf{SF} &\equiv \left(\frac{M_{\mathrm{obs}_{S_1}}}{M_{0S_1}}, \frac{M_{\mathrm{obs}_{S_2}}}{M_{0S_2}}, \ldots, \frac{M_{\mathrm{obs}_{S_N}}}{M_{0S_N}}\right) \\ &= \mathbf{M}_0^{-1}(\mathbf{I} - e^{\mathbf{A}\,\mathrm{TR}}\cos\theta)^{-1}(\mathbf{I} - e^{\mathbf{A}\,\mathrm{TR}})\mathbf{M}_0 \sin\theta, \end{aligned} \qquad [5]$$

where the matrix $\mathbf{A}$ is a function of all T_1's and rate constants within the exchange network. Thus, in the presence of CE, the SF of a resonance depends upon the T_1's and M_0's of all species in the exchange network as well as upon the rate constants.

Definition of Quantitation Errors

Consider an NMR experiment with a control period (Ctl) followed by an intervention period (Int); this can also represent system changes secondary to, for example, instabilities (*4*). The typical method of correcting for saturation of a resonance is to first determine $\mathrm{SF}^{\mathrm{Ctl}}$ from long TR and short TR experiments (Eq. [2]). During Int, only short TR spectra are obtained in order to improve S/N; $\mathrm{SF}^{\mathrm{Int}}$ is neither measured nor calculated. By definition of $\mathrm{SF}^{\mathrm{Int}}$, the true fully relaxed magnetization during Int, M_0^{Int}, is correctly given by:

$$M_0^{\mathrm{Int}} = \frac{M_{\mathrm{obs}}^{\mathrm{Int}}}{\mathrm{SF}^{\mathrm{Int}}}. \qquad [6]$$

However, lacking $\mathrm{SF}^{\mathrm{Int}}$, the fully relaxed magnetization during Int is calculated using $\mathrm{SF}^{\mathrm{Ctl}}$:

$$M_0^{\mathrm{Int},Apparent} = \frac{M_{\mathrm{obs}}^{\mathrm{Int}}}{\mathrm{SF}^{\mathrm{Ctl}}} \qquad [7]$$

Clearly, $M_0^{\mathrm{Int}} = M_0^{\mathrm{Int},Apparent}$ if and only if

$$\mathrm{SF}^{\mathrm{Ctl}} = \mathrm{SF}^{\mathrm{Int}}. \qquad [8]$$

Otherwise, there is an error in quantitation, which we define as:

$$\%\ \text{error in}\ M_0^{\mathrm{Int},Apparent} = \frac{\left[M_0^{\mathrm{Int},Apparent} - M_0^{\mathrm{Int}}\right]}{M_0^{\mathrm{Int}}} \times 100\%. \qquad [9]$$

SIMULATION METHODS

Simulation parameters for the system described in Eq. [3] are given in Table 1. Note that no single reference provides all of the required parameters for a given simulation.

Simulation Parameter Selection for Hearts

Metabolite concentrations for control and ischemic hearts were taken from a study by Kalil-Filho *et al.* (*7*) with TR = 2.1 s

TABLE 1
Physiological Parameters Used for the Model Simulations

	T_1(PCr)	$T_1(\gamma$-ATP)	$T_1(P_i)$	M_0(PCr)	$M_0(\beta$-ATP)	$M_0(P_i)$	$k_{\mathrm{PCr}\to\gamma\text{-ATP}}$	$k_{\mathrm{P_i}\to\gamma\text{-ATP}}$
Heart								
Control	2.78[9]	0.64[9]	2.40[9]	1.00[7]	0.62[7]	0.23[7]	0.70[8]	0.37[9]
Ischemia	**2.22**	**0.50**	**3.60**	0.05[7]	0.03[7]	2.78[7]	0.20[8]	**0.11**
Skeletal								
Control	6.30[6]	2.50[6]	4.00[6]	1.00[10]	0.23[10]	0.07[10]	0.21[6]	**0.11**
Stimulation	**5.00**	**2.00**	**6.00**	0.29[10]	0.16[10]	0.54[10]	0.32[6]	**0.16**
Brain								
Control	5.00[13]	1.40[13]	3.00[13]	1.00[11]	2.10[11]	1.26[11]	0.26[12]	0.18[13]
Seizure	**4.00**	**1.10**	**4.50**	0.65[12]	2.00[12]	2.40[12]	0.13[12]	**0.09**

Note. Values in bold are estimates calculated as described in the study. All other values were obtained from the literature.

and $\theta = 60^\circ$; this flip angle was chosen according to Eq. [2.5] for PCr. $k_{\text{PCr}\rightarrow\gamma\text{-ATP}}$ for control and ischemic hearts were taken from a study by Neubauer *et al.* (*8*). T_1^{Ctl}(PCr), $T_1^{\text{Ctl}}(\gamma$-ATP), and $T_1^{\text{Ctl}}(\text{P}_\text{i})$ and $k_{\text{P}_\text{i}\rightarrow\gamma\text{-ATP}}$ were obtained from Spencer *et al.* (*9*).

Simulation Parameter Selection for Skeletal Muscle

Metabolite concentrations were taken from Cieslar and Dobson (*10*), who used TR = 1.0 s and $\theta = 90^\circ$. $k_{\text{PCr}\rightarrow\gamma\text{-ATP}}$ during Ctl and metabolite T_1^{Ctl}'s were taken from a study by Horska *et al.* (*6*).

Simulation Parameter Selection for Brain

Control metabolite concentrations were obtained from Young *et al.* (*11*). $k_{\text{PCr}\rightarrow\gamma\text{-ATP}}$ and metabolite concentrations pre- and postseizure were taken from Holtzman *et al.* (*12*), who used TR = 10 s and $\theta = 90^\circ$, consistent with the Ernst angle optimization of S/N. This TR was selected to avoid partial saturation. T_1^{Ctl}(PCr), $T_1^{\text{Ctl}}(\gamma$-ATP), and $T_1^{\text{Ctl}}(\text{P}_\text{i})$, and $k_{\text{P}_\text{i}\rightarrow\gamma\text{-ATP}}$ were obtained from Shoubridge *et al.* (*13*).

Values for $k^{\text{Int}}_{\text{P}_\text{i}\rightarrow\gamma\text{-ATP}}$ in ischemic heart and seizing brain were not available. Accordingly, they were estimated by assuming that the ratio $\alpha = k^{\text{Ctl}}_{\text{PCr}\rightarrow\gamma\text{-ATP}}/k^{\text{Ctl}}_{\text{P}_\text{i}\rightarrow\gamma\text{-ATP}}$ was the same during Ctl and Int. In skeletal muscle, for which neither control nor stimulation values of $k_{\text{P}_\text{i}\rightarrow\gamma\text{-ATP}}$ were available, α was assumed to be equal to 2. Values of T_1^{Int} used in the simulations incorporating changing T_1's were obtained by assuming similar percentage changes as those reported by Newcomer and Boska (*14*) in exercising human skeletal muscle, in which T_1(PCr) and $T_1(\beta$-ATP) decreased by 20% while $T_1(\text{P}_\text{i})$ increased by over 50%. Values which were based upon the assumptions noted above are bold in Table 1. Although $T_1(\gamma$-ATP) was not found to vary in Ref. (*14*), we have nevertheless evaluated the consequences of changes in $T_1(\gamma$-ATP) on the order of those observed for $T_1(\beta$-ATP) in Ref. (*14*).

Mathematica (Wolfram Research, Inc., Champaign, IL) was used for all simulations. Constrained optimization was used to determine the values of TR and θ which resulted in the maximal root-mean-square of the S/N for PCr, β-ATP, and P_i subject to upper bounds of 5 and 10% on the maximum systematic error in quantitation of all metabolites according to Eq. [9]. Simulations were performed separately for T_1 remaining the same, and T_1 changing, between Ctl and Int. The expression for S/N per unit time follows directly from the definition of SFs and is

$$S/N \propto \text{SF}/\sqrt{\text{TR}}. \qquad [10]$$

As the SF in Eq. [10] we used the SF^{Ctl}, reflecting the common experimental practice in which the S/N is maximized under control conditions. The systematic error and the S/N resulting from the optimization were compared with the corresponding values resulting from use of particular literature values of TR and θ. Note that the optimization algorithm produced values of TR and θ with maximal root-mean-squared S/N for the given error bound, so that the errors were often below the specified bounds of 5 and 10%.

Simulations were also performed to individually determine the dependence of errors in $M_0^{\text{Int},Apparent}$(PCr) on M_0^{Int}(PCr), $k^{\text{Int}}_{\text{PCr}\rightarrow\gamma\text{-ATP}}$, and T_1^{Int}(PCr). Results were generated for five pairs of TR and θ. These were: (i) literature values as cited above; (ii) and (iii) short TR, 0.25 s, and long TR, 30 s, with the literature θ; (iv) and (v) results generated from the optimizations with 5 and 10% error bounds. Finally, an analysis of the relationship between quantitation error and the S/N of PCr as a function of TR and θ was performed, assuming $T_1^{\text{Ctl}} = T_1^{\text{Int}}$ for all species. These results are presented as contour plots permitting the direct visualization of the tradeoff inherent in the goals of maximizing S/N while minimizing errors.

All simulation results should be regarded as representative only, due to the wide range of possible experimental and chemical parameters.

SIMULATION RESULTS

Heart

Constrained optimization of TR and θ. Table 2a shows the values of TR and θ which maximize the root-mean-squared S/N per unit time under the constraints of 5 and 10% maximum error due to CE for PCr, β-ATP, and P_i. $T_1^{\text{Ctl}} = T_1^{\text{Int}}$ for all species is assumed. Results are also provided for the literature values of TR and θ. The literature values generated the greatest errors but also the largest S/N; the maximum error, −14%, was for PCr. The S/N cost of reduced error was substantial, with the greatest loss being seen in β-ATP at the 5% error bound. Errors due to CE were zero for β-ATP since it is modeled as undergoing no exchange.

TABLE 2a
Calculated TR and θ for Optimal S/N of All Metabolites with Constraint of 5 and 10% on Quantitation Error

			PCr		β-ATP		P_i	
	TR (s)	θ	S/N	(% error)	S/N	(% error)	S/N	(% error)
Heart								
5%	6.30	76°	0.76	(−5.00)	0.71	(0.00)	0.78	(−3.43)
10%	0.65	26°	0.89	(−10.0)	0.90	(0.00)	0.90	(−6.24)
Literature	2.10	60°	1.00	(−14.4)	1.00	(0.00)	1.00	(−9.02)
Skeletal muscle								
5%	0.65	31°	1.90	(5.00)	1.30	(0.00)	1.57	(1.17)
10%	0.55	30°	1.90	(5.11)	1.32	(0.00)	1.60	(1.18)
Literature	1.00	90°	1.00	(4.46)	1.00	(0.00)	1.00	(0.87)
Brain								
5%	0.71	26°	1.19	(−5.00)	1.39	(0.00)	1.27	(−1.56)
10%	0.50	38°	1.19	(−8.15)	1.76	(0.00)	1.38	(−2.70)
Literature	10.0	90°	1.00	(−2.60)	1.00	(0.00)	1.00	(−0.52)

Note. T_1's of all metabolites are fixed between Ctl and Int. The S/N values are normalized to the S/N calculated from the literature values of TR, θ.

TABLE 2b
Calculated TR and θ for Optimal S/N of All Metabolites with Constraint of 5 and 10% on Quantitation Errors

			PCr		β-ATP		P_i	
	TR (s)	θ	S/N	(% error)	S/N	(% error)	S/N	(% error)
Heart								
5%	9.35	79°	0.64	(−2.39)	0.59	(0.00)	0.66	(−5.00)
10%	6.27	72°	0.75	(−4.85)	0.70	(0.00)	0.76	(−10.00)
Literature	2.10	60°	1.00	(−10.9)	1.00	(1.10)	1.00	(−23.0)
Skeletal muscle								
5%	8.71	72°	1.73	(5.00)	1.06	(1.28)	1.31	(−3.67)
10%	1.91	43°	1.90	(10.0)	1.24	(5.67)	1.53	(−8.75)
Literature	1.00	90°	1.00	(26.1)	1.00	(19.3)	1.00	(−25.2)
Brain								
5%	7.50	69°	1.05	(−0.29)	1.07	(0.22)	1.06	(−5.00)
10%	2.02	42°	1.18	(0.76)	1.35	(2.74)	1.25	(−10.0)
Literature	10.0	90°	1.00	(−0.41)	1.00	(0.07)	1.00	(−4.06)

Note. T_1^{Int}'s of PCr and γ-ATP are decreased by 20% and P_i is increased by 50% from their respective Ctl value. The S/N values are normalized to the S/N calculated from the literature values of TR, θ.

When T_1's were allowed to differ between Ctl and Int (Table 2b), the maximum error, −23%, was for P_i. This was due to the relatively large change in $T_1(P_i)$. Significant reductions in S/N are again seen to occur for TR and θ choices resulting in the specified bounds. For β-ATP, the S/N is reduced nearly by a factor of two for a 5% bound on maximal error.

The optimized values of TR and θ were similar between the T_1 fixed and the T_1 variable cases for the 5% error bound, but were very different for the 10% error bound.

Chemical dependency. Figure 1 illustrates the dependence on chemical parameters of the percentage error in $M_0^{Int,Apparent}$(PCr) with respect to M_0^{Int}(PCr), $k^{Int}_{PCr\rightarrow\gamma\text{-ATP}}$, and T_1^{Int}(PCr). While the *changes* in this error with respect to M_0^{Int}(PCr) and $k^{Int}_{PCr\rightarrow\gamma\text{-ATP}}$ over the range displayed were small, the errors themselves were substantial, on the order of −15% for $M_0^{Int,Apparent}$(PCr) for the literature values of TR and θ. There was a strong dependence of errors upon TR, with minimum errors for long TR and for TR → 0 (data overlying TR = 30 curve) and maximum errors for a short TR of 0.25 s. These results are in accord with Ref. (*3*, Figs. 8–10). The dependency and the absolute magnitude of the errors with respect to T_1^{Int}(PCr) variations are somewhat larger than for variations in M_0^{Int}(PCr) or $k^{Int}_{PCr\rightarrow\gamma\text{-ATP}}$. We note that the zero-error point of intersection of the curves in Fig. 1c would be identically equal to the control value of T_1(PCr) were it not for the change in the other system parameters between Ctl and Int.

Simulations with $T_1^{Ctl} = T_1^{Int} = 2$ times the control T_1 values given in Table 1, with pulse parameters TR = 2.1 s and $\theta = 60°$, demonstrate an increase in error from −14 (Table 2a, literature T_1's) to −24% for PCr and from −9 to −16% for P_i. Simulations with these same doubled T_1's, but with pulse parameters of TR = 2.0 s and $\theta = 90°$, yield an error of −32 and −21% for PCr and P_i, respectively.

Skeletal Muscle

Constrained optimization of TR and θ. For the literature values of pulse parameters chosen, TR = 1.0 s and $\theta = 90°$, errors were substantially less for skeletal muscle than for heart when T_1's are constant (Table 2a). The maximum error, for PCr, was 4.5%. However, these parameters yielded significantly lower S/N than did the values determined from the optimization. For PCr, the S/N was nearly doubled with the optimal TR and θ choices as compared with the literature values. S/N was essentially unchanged when the error bound was increased from 5 to 10%. Errors were substantially larger when T_1's varied (Table 2b), with a maximum value, again seen for PCr, of 26% using the literature TR and θ. S/N was markedly increased by use of pulse parameters determined from the optimization.

The optimal values of TR and θ were similar between the T_1 fixed and the T_1 variable cases for the 10% error bound, but were very different for the 5% error bound.

Chemical dependency. Figure 2 shows error dependence on parameters. The overall magnitude of the errors is somewhat smaller than for heart, while the dependence of errors with respect to M_0^{Int}(PCr) over the range shown was greater. Large errors are seen for intermediate values of TR. For the smallest values of $k^{Int}_{PCr\rightarrow\gamma\text{-ATP}}$ (Fig. 2b), the maximum absolute errors for literature values of TR and θ are approximately −8%, and reach 20–25% for $k^{Int}_{PCr\rightarrow\gamma\text{-ATP}}$ on the order of 1 s^{-1} (results not shown). Over the range of T_1^{Int}(PCr) illustrated, errors increased rapidly as T_1^{Int}(PCr) decreased.

Simulations with $T_1^{Ctl} = T_1^{Int} = 2$ times the control T_1 values given in Table 1 and, using the literature values for the pulse parameters of TR = 1.0 s and $\theta = 90°$, yield an error in PCr which is essentially unchanged from the 4.5% given in Table 2a. With these same literature pulse parameters and using $T_1^{Ctl} = T_1^{Int}$ = the control T_1 values given in Table 1, if the forward CK rate constant increases from $k^{Ctl}_{PCr\rightarrow\gamma\text{-ATP}} = 0.21$ s^{-1} to $k^{Int}_{PCr\rightarrow\gamma\text{-ATP}} = 0.71$ s^{-1}, that is, if it undergoes the same magnitude of change as in the heart simulations, the percentage error for PCr increases from 4.5 to 14%.

Brain

Constrained optimization of TR and θ. Results obtained with the literature values of TR = 10 s and $\theta = 90°$ demonstrate that use of a long TR will reduce errors when correcting for partial saturation. The largest error was −2.6%, seen for PCr. For fixed T_1, with the pulse parameters resulting from the optimization with the 10% error constraint, the error in PCr was three times higher but the S/N was increased by 20%.

When T_1's were allowed to vary, the maximum error, −4.1%, was for P_i when using the literature pulse parameters. Errors for P_i and for PCr approximately doubled, but S/N increased by 20%, for the parameters derived from a 10% error bound optimization.

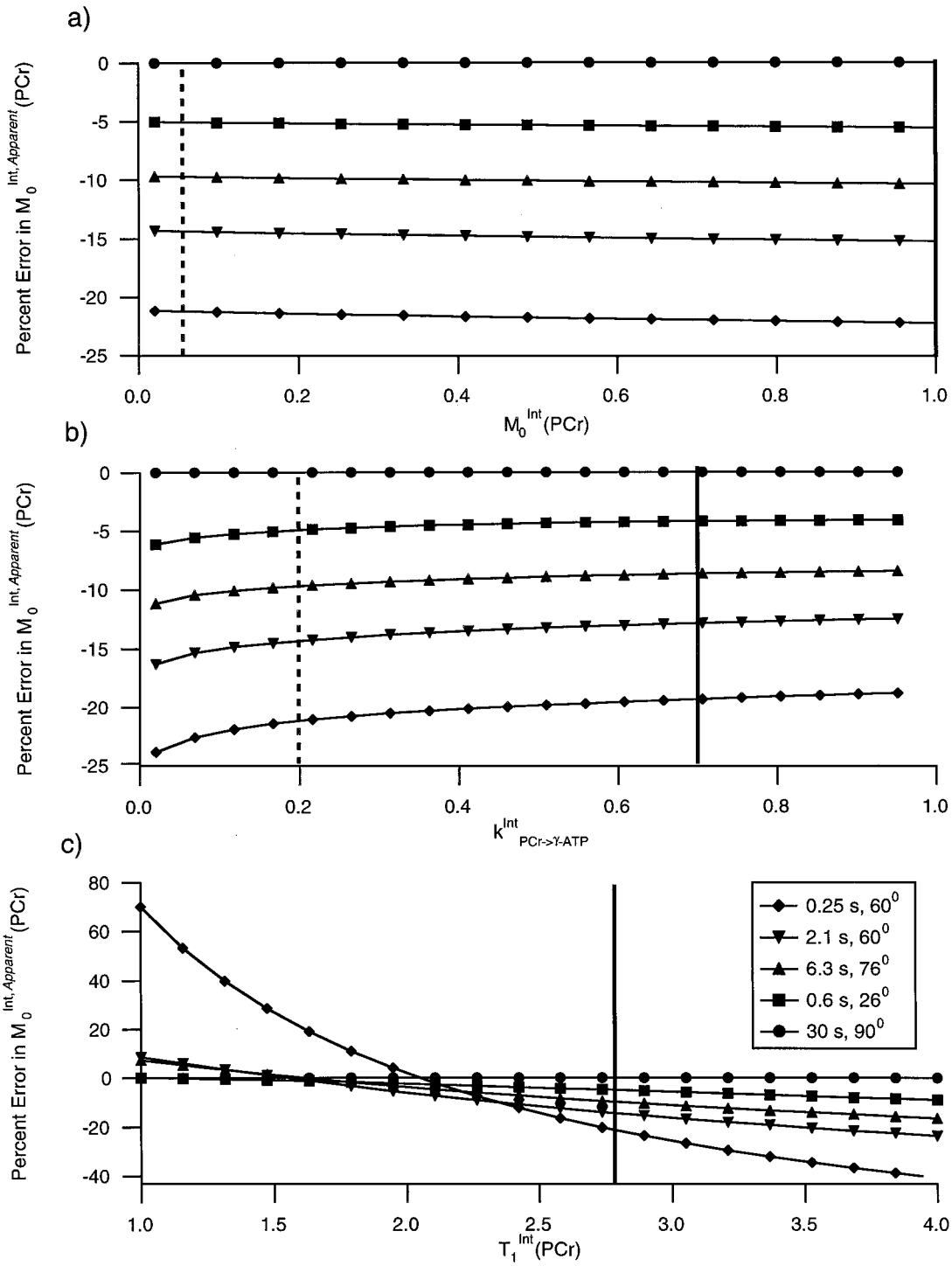

FIG. 1. Analyses of the dependence of systematic errors in $M_0^{\mathrm{Int},Apparent}$(PCr) on changes in M_0^{Int}(PCr), $k^{\mathrm{Int}}_{\mathrm{PCr}\rightarrow\gamma\text{-ATP}}$, and T_1^{Int}(PCr) for five sets of TR and θ. Except for the independent variable, the parameters used were those for heart muscle presented in Table 1, with $T_1^{\mathrm{Int}} = T_1^{\mathrm{Ctl}}$ for all metabolites except for the changes in T_1^{Int}(PCr) explicitly evaluated in panel C. The Ctl and Int values of the independent variable as used in the optimizations illustrated in Table 2 are denoted by the solid and dashed vertical lines, respectively, for reference.

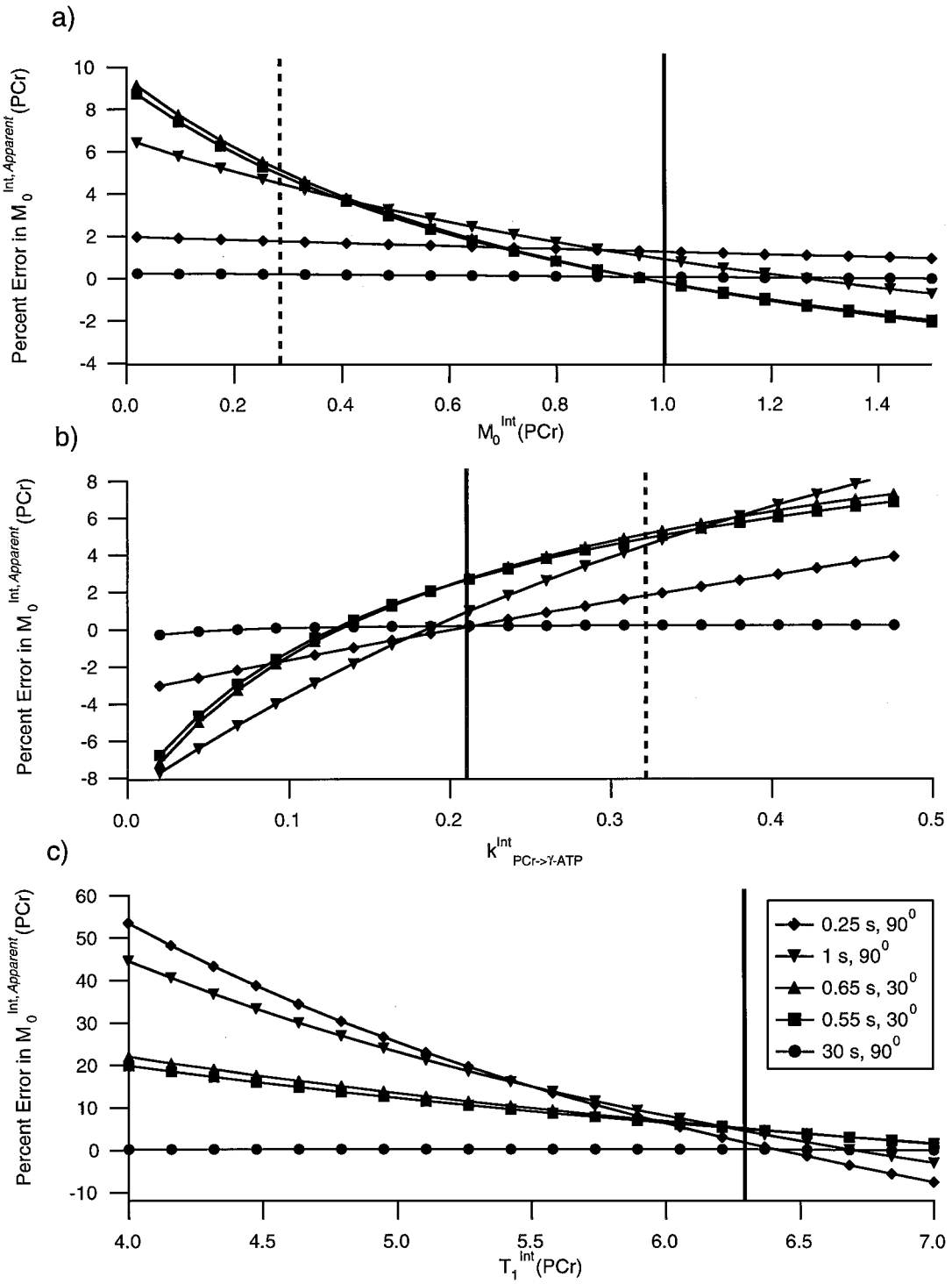

FIG. 2. Similar to Fig. 1, except with use of parameters for skeletal muscle.

Chemical dependency. Trends with respect to changes in M_0^{Int}(PCr) are similar to those seen for heart (Fig. 3a); Fig. 3b shows that trends with respect to changes in $k^{\text{Int}}_{\text{PCr}\rightarrow\gamma\text{-ATP}}$ are similar to those seen for skeletal muscle. While the changes in the errors with respect to M_0^{Int}(PCr) over the range displayed were small, the errors themselves were substantial. Both a significant dependence of error on $k^{\text{Int}}_{\text{PCr}\rightarrow\gamma\text{-ATP}}$ over the particular range illustrated and large overall errors due to differences between $k^{\text{Ctl}}_{\text{PCr}\rightarrow\gamma\text{-ATP}}$ and $k^{\text{Int}}_{\text{PCr}\rightarrow\gamma\text{-ATP}}$ were seen. As is also evident from Table 2a, the literature values of TR and θ resulted in a

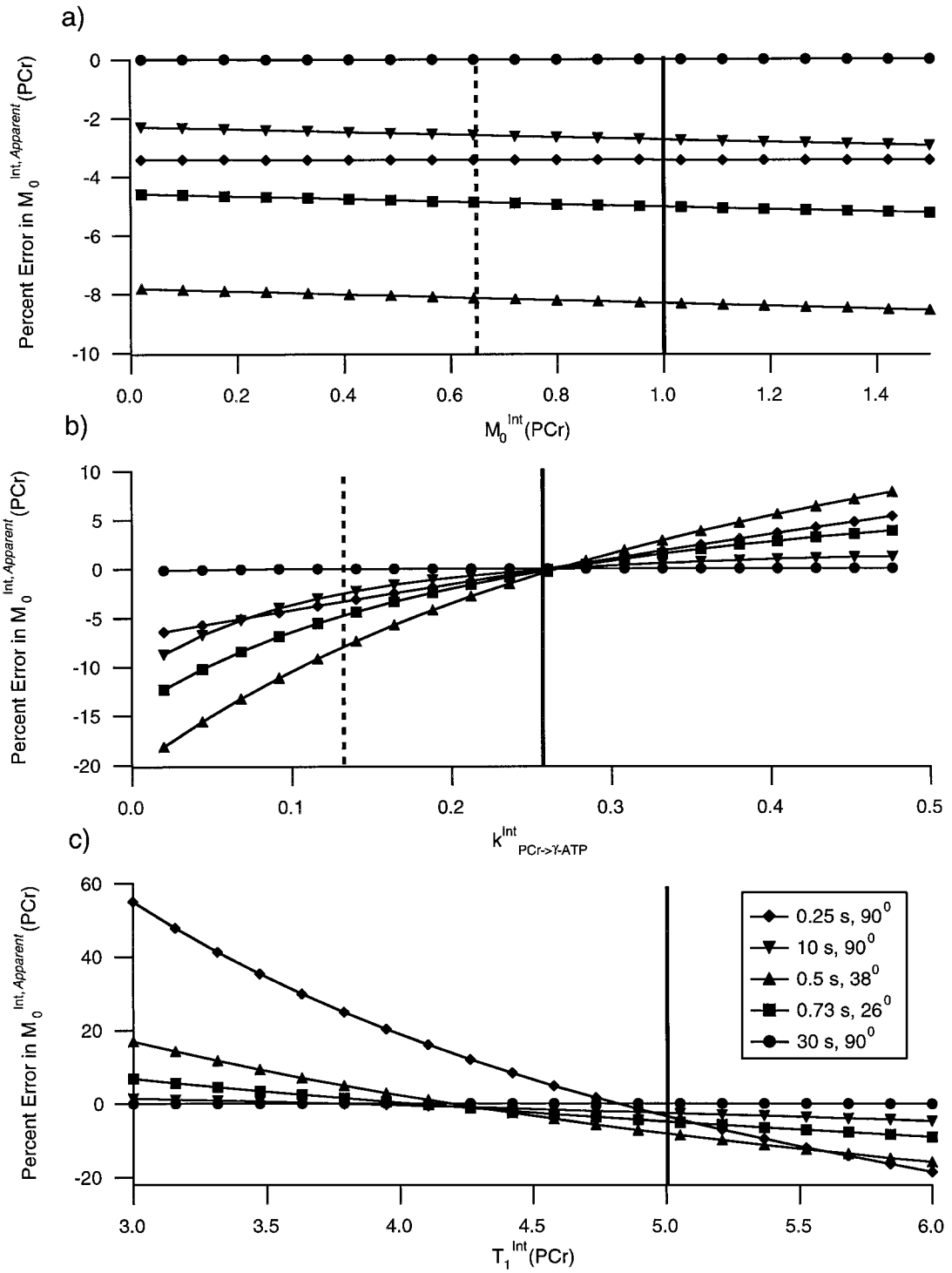

FIG. 3. Similar to Fig. 1, except with use of parameters for brain.

small systematic error, on the order of 1%. However, Fig. 3b demonstrates that if $k^{\text{Int}}_{\text{PCr}\rightarrow\gamma\text{-ATP}}$ becomes substantially smaller than $k^{\text{Ctl}}_{\text{PCr}\rightarrow\gamma\text{-ATP}}$, even a long TR of 10 s can give large errors. Again, larger errors were seen for smaller values of T_1^{Int}(PCr).

If TR = 2.0 s and $\theta = 90^\circ$ are used as pulse parameters, the quantitation error for PCr is -10%, rather than the -2.6% seen with the literature value of TR = 10 s, $\theta = 90^\circ$. If, in addition to this change in pulse parameters, $T_1^{\text{Ctl}} = T_1^{\text{Int}} = 2$ times the

control T_1 values given in Table 1, the error in PCr increases only slightly, to -12%. Maintaining these T_1's but reverting to the literature values for the pulse parameters results in a -6.4% error. With these same parameters but using the CK rate constants found in the heart, the error in PCr increases to -24%.

Consequences of Pulse Parameter Choices

The particular literature values for TR and θ analyzed above are in no way standard for study of a particular tissue type. Variables which may influence choice of pulse parameters are magnetic field strength, tissue type, interventions, the tradeoff between temporal resolution and quantitation accuracy, and specific interest in a single line within a spectrum. Accordingly, we investigated a wide range of TR and θ with respect to S/N and quantitation error. All results presented in this section are for $T_1^{\mathrm{Ctl}} = T_1^{\mathrm{Int}}$.

Figure 4 is a contour plot of percentage errors in PCr quantitation, and S/N normalized to that resulting from use of the literature values, for the heart as a function of TR and θ. As expected, an increase in TR tends to reduce error but also reduces S/N . Examination of the region within the $S/N = 1$ contour shows that greater S/N than for the literature values of TR $= 2.1$ s, $\theta = 60^\circ$ can be obtained but only with a substantial loss of accuracy. It is also readily seen that a maximum S/N of only approximately 0.75 with respect to the literature results is achievable when constraining error below 5%. If the error bound is increased to 10% then S/N of 0.9 is achievable using a wide variety of TR and θ combinations, varying essentially linearly from 1 s, 32° to 3.5 s, 67°.

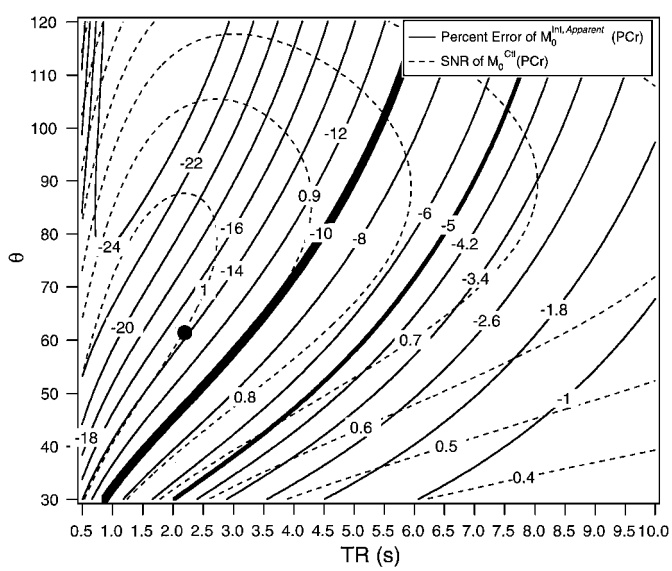

FIG. 4. Contour plot of the percentage error in $M_0^{\mathrm{Int},Apparent}$(PCr) and S/N of PCr as a function of TR and θ using heart parameters. $T_1^{\mathrm{Int}} = T_1^{\mathrm{Ctl}}$ was assumed for all metabolites. Solid lines: percentage error. Dashed lines: S/N, normalized to the value of S/N resulting from the use of the literature TR and θ. Five and 10% error contours are designated by heavily weighted lines. Literature values for TR and θ are represented by a dot.

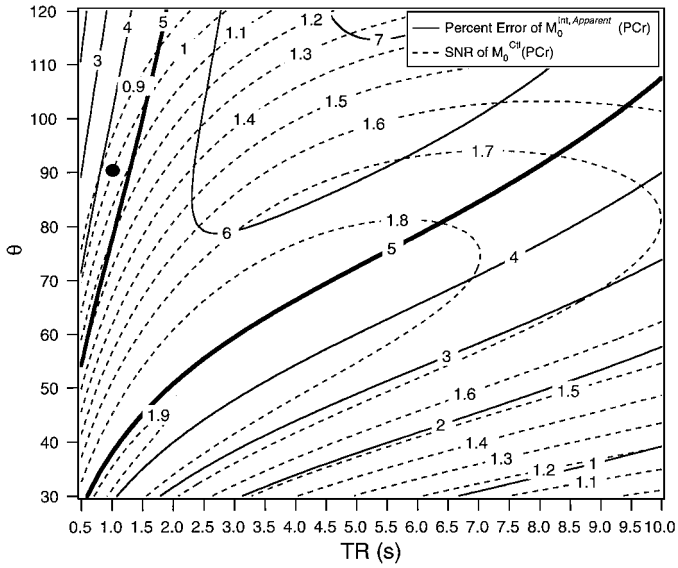

FIG. 5. Similar to Fig. 4, only for skeletal muscle parameters.

Figure 5 is a contour plot similar to that of Fig. 4 but for skeletal muscle. Note that there is no boundary for error at 10%, consistent with the results shown in Table 2a. It is apparent that there is a wide variety of TR and θ that yield a small error, on the order of a few percentage points, as well as S/N substantially greater than that resulting from use of the literature parameters.

Figure 6 is a similar contour plot for brain. It is evident that if a constraint of 5% is imposed on the error, then it is difficult to significantly improve the S/N over that yielded by the literature values. Further, relaxing the error constraint to 10% does not permit a substantial increase in S/N.

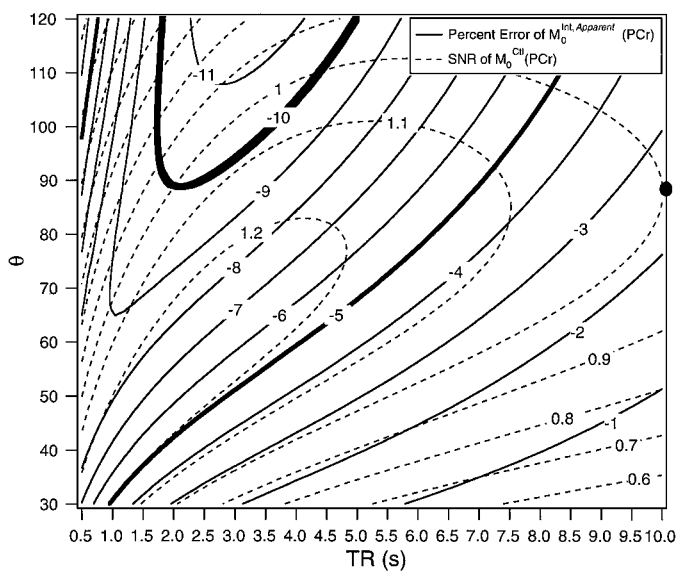

FIG. 6. Similar to Fig. 4, only for brain parameters.

DISCUSSION

The magnitude of systematic errors generated by the usual procedure for correcting for partial saturation in biological samples undergoing an intervention was described for heart, skeletal muscle, and brain, using representative parameters values from the literature. Specific numerical results will differ depending upon the selection of values as simulation inputs, and the particulars of an experimental protocol will determine the magnitude of the errors in practice.

For unchanging T_1's, the optimization algorithm yielded small values for TR and θ for skeletal muscle and brain, both of which, according to the illustrative parameters we have selected, have relatively large T_1's and relatively small changes in rate constant. CE plays a larger role when a larger change in rates occurs, as was the case for heart. For the 5% error bound, optimal TR and θ were substantially larger for heart than for skeletal muscle and brain.

Varying T_1's between periods further increased the magnitude of the systematic error. Thus, although percentage changes in T_1 secondary to an intervention may be significantly less than changes in concentrations or rate constants (*6, 13*), these small changes may still contribute significantly to quantitation error.

The optimization analysis demonstrates that accurate measurements may in principle be performed without large sacrifices in S/N and perhaps even with improvements in S/N, as compared to ad hoc choices of pulse parameters. In common with many other optimization algorithms, precise implementation of this approach requires knowledge of the full set of chemical parameters of the experiment at the outset. However, some of these values, such as M_0^{Int}, may not be known until the experiment is actually performed, and others, such as T_1's and reaction rates, may never be ascertained in a given protocol. Thus, values for the simulation input parameters must be estimated from a priori knowledge. Our results indicate to what extent uncertainty in certain postintervention parameters will influence errors. After estimation of appropriate TR and θ, the investigator may wish to empirically increase TR to ensure that the error resulting from SF correction remains below a set threshold.

The difficulty in selecting pulse parameters is evident in Table 2a, where a large difference is seen in the values of TR and θ for the 5 and 10% error bounds for heart. However, these optima are rather broad and yield S/N close to that of a global optimum. Figures 4–6 illuminate this. In the case of heart, for example, while TR = 6.3 s, $\theta = 76^\circ$ is optimal for the 5% error constraint, and TR = 0.65 s, $\theta = 26^\circ$ is optimal for the 10% error constraint, one could start from the 5% constraint optimal values, maintaining θ, and decrease TR until the 10% error contour is reached, and achieve a S/N of 0.87 which is not very different from the true optimal value of 0.90. Further, the opposite procedure, that is, starting from the 10% bound optimal pulse parameters and increasing TR to its point of intersection with the 5% contour yields a S/N of 0.67, which, while substantially less than the optimal $S/N = 0.76$, is nevertheless still within a reasonable range. Knowledge of these local optima derived from the appropriate contour plot allows a TR and θ to be chosen which is appropriate for particular objectives, such as maximizing joint S/N or the S/N of a particular resonance, minimizing chemical exchange effects, minimizing saturation of a specific resonance, or working within instrumental limitations.

For all biological systems investigated here, separate calculations demonstrated that the overall errors in the ratio $M_0^{\mathrm{Int},Apparent}(\mathrm{PCr})/M_0^{\mathrm{Int},Apparent}(\mathrm{P_i})$ due to changes in $M_0^{\mathrm{Int}}(\mathrm{PCr})$, $k^{\mathrm{Int}}_{\mathrm{PCr}\rightarrow\gamma\text{-ATP}}$, and $T_1^{\mathrm{Int}}(\mathrm{PCr})$ lead to errors approximately of magnitude 40–60% of those in $M_0^{\mathrm{Int},Apparent}(\mathrm{PCr})$. However, for small $T_1^{\mathrm{Int}}(\mathrm{PCr})$ the errors in the ratio become approximately twice those of the errors in $M_0^{\mathrm{Int},Apparent}(\mathrm{PCr})$.

T_1's are complex functions of magnetic field strength, tissue edema and vascularity, presence of relaxation agents, temperature, and myriad other factors. Metabolite level changes depend upon, for example, degree of metabolic stress and its reversal, substrate supplementation, and duration of intervention. Reaction rates depend upon such variables as bioenergetic status, temperature, substrate concentrations, workload, and enzymatic manipulations through transgenic techniques. Hence quantitation errors of the type considered here must be considered not only in terms of currently published paradigms, but also with respect to particular parameter values and changes in these values as novel experiments are performed.

Our analysis has been explicitly presented in terms of the one-pulse sequence. The results are also applicable to variations of this experiment, incorporating, for example, spatial localization or spectral editing into this basic sequence, as long as partially saturated spectra are obtained. Similarly, our results have been presented in terms of a single NMR experiment in which the sample is perturbed, leading to changes in its chemical parameters. However, identical considerations apply to the case in which SFs are measured in one group of subjects or samples and are then applied to correct for partial saturation in a different group for which chemical parameters may be different.

REFERENCES

1. R. R. Ernst and W. A. Anderson, Application of Fourier transform spectroscopy to magnetic resonance, *Rev. Sci. Instrum.* **37,** 93–102 (1966).
2. R. G. S. Spencer, J. A. Ferretti, and G. H. Weiss, NMR saturation factors in the presence of chemical exchange, *J. Magn. Reson.* **84,** 223–235 (1989).
3. R. G. S. Spencer and K. W. Fishbein, Measurement of spin-lattice relaxation times and concentrations in systems with chemical exchange using the one-pulse sequence: breakdown of the Ernst model for partial saturation in nuclear magnetic resonance spectroscopy, *J. Magn. Reson.* **142,** 120–135 (2000).
4. R. G. S. Spencer, K. W. Fishbein, and C. J. Galban, Pitfalls in the measurement of metabolite concentrations using the one-pulse experiment in in vivo NMR: Commentary on "On neglecting chemical exchange effects when correcting in vivo 31P-MRS data for partial saturation," *J. Magn. Reson.* **149,** 251–257 (2001).
5. A. Horska, J. Horsky, and R. G. S. Spencer, Measurement of spin–lattice relaxation times in systems undergoing chemical exchange, *J. Magn. Reson. A.* **110,** 82–89 (1994).

6. A. Horska and R. G. S. Spencer, Measurement of spin-lattice relaxation times and kinetic rate constants in rat muscle using progressive partial saturation and steady-state saturation transfer, *Magn. Reson. Med.* **36,** 232–240 (1996).

7. R. Kalil-Filho, G. Gerstenblith, R. G. Hansford, V. P. Chacko, K. Vandegaer, and R. G. Weiss, Regulation of myocardial glycogenolysis during postischemic reperfusion, *J. Mol. Cell. Cardiol.* **23,** 1467–1479 (1991).

8. S. Neubauer, B. L. Hamman, S. B. Perry, J. A. Bittl, and J. S. Ingwall, Velocity of the creatine kinase reaction decreases in postischemic myocardium: a 31P-NMR magnetization transfer study of the isolated ferret heart, *Circ. Res.* **63,** 1–15 (1988).

9. R. G. S. Spencer, J. A. Balschi, J. S. Leigh, Jr., and J. S. Ingwall, ATP synthesis and degradation rates in the perfused rat heart. 31P-nuclear magnetic resonance double saturation transfer measurements, *Biophys J.* **54,** 921–929 (1988). [Erratum: *Biophys. J.* **54,** 1186 (1988)].

10. J. H. Cieslar and G. P. Dobson, Free [ADP] and aerobic muscle work follow at least second order kinetics in rat gastrocnemius in vivo, *J. Biol. Chem.* **275,** 6129–6134 (2000).

11. R. S. Young, M. D. Osbakken, R. W. Briggs, S. K. Yagel, D. W. Rice, and S. Goldberg, 31P-NMR study of cerebral metabolism during prolonged seizures in the neonatal dog, *Ann. Neurol.* **18,** 14–20 (1985).

12. D. Holtzman, M. Offutt, M. Tsuji, L. J. Neuringer, and D. Jacobs, Creatine kinase-catalyzed reaction rate in the cyanide-poisoned mouse brain, *J. Cereb. Blood Flow Metab.* **13,** 153–161 (1993).

13. E. A. Shoubridge, R. W. Briggs, and G. K. Radda, 31P-NMR saturation transfer measurements of the steady state rates of creatine kinase and ATP synthetase in the rat brain, *FEBS Lett.* **140,** 289–292 (1982).

14. B. R. Newcomer and M. D. Boska, T1 measurements of 31P metabolites in resting and exercising human gastrocnemius/soleus muscle at 1.5 Tesla, *Magn. Reson. Med.* **41,** 486–494 (1999).